# The Musculature That Drives Active Touch by Vibrissae and Nose in Mice

SEBASTIAN HAIDARLIU,[1]* DAVID KLEINFELD,[2] MARTIN DESCHÊNES,[3] AND EHUD AHISSAR[1]

[1]Department of Neurobiology, The Weizmann Institute of Science, Rehovot, Israel
[2]Department of Physics and Section of Neurobiology, University of California at San Diego, La Jolla, California
[3]Department of Psychiatry and Neuroscience, Faculty of Medicine, Laval University, Québec City, Canada

ABSTRACT

Coordinated action of facial muscles during whisking, sniffing, and touching objects is an important component of active sensing in rodents. Accumulating evidence suggests that the anatomical schemes that underlie active sensing are similar across the majority of whisking rodents. Intriguingly, however, muscle architecture in the mystacial pad of the mouse was reported to be different, possessing only one extrinsic vibrissa protracting muscle (M. nasalis) in the rostral part of the snout. In this study, the organization of the muscles that move the nose and the mystacial vibrissae in mice was re-examined and compared with that reported previously in other rodents. We found that muscle distribution within the mystacial pad and around the tip of the nose in mice is isomorphic with that found in other whisking rodents. In particular, in the rostral part of the mouse snout, we describe both protractors and retractors of the vibrissae. Nose movements are controlled by the M. dilator nasi and five subunits of the M. nasolabialis profundus, with involvement of the nasal cartilaginous skeleton as a mediator in the muscular effort translation. Anat Rec, 00:000–000, 2015. © 2014 Wiley Periodicals, Inc.

**Key words: vibrissa; rhinarium; facial musculature; active touch; rodents**

Sensory organ movement supports active sensing in different modalities (Ahissar and Arieli, 2001; Mitchinson et al., 2011; Venkatraman and Carmena, 2011; Stamper et al., 2012). Orofacial behaviors involve active odor sensing (sniffing; Welker, 1964; Kepecs et al., 2006; Wachowiak, 2011), active vibrissal touch (whisking; Welker, 1964; Kleinfeld et al., 2006; Ahissar and Knutsen, 2008; Prescott et al., 2011; Maravall and Diamond, 2014), and active gustatory sampling (licking; Grill and Norgren, 1978; Katz et al., 2001; Bahar et al., 2004).

Abbreviations used: CCO = cytochrome oxidase; DNC = dorsal nasal cartilage; MP = mystacial pad; NCS = nasal cartilaginous skeleton

Grant sponsor: The Minerva Foundation funded by the Federal German Ministry for Education and Research; Grant sponsor: United States National Institutes of Health; Grant number: NS058668; Grant sponsor: United States National Science Foundation; Grant number: PHY-1451026; Grant sponsor: United States–Israel Binational Science Foundation; Grant number: 2011432; Grant sponsor: NSF-BSF Brain Research EAGER program; Grant number: 2014906; Grant sponsor: The Canadian Institutes of Health Research; Grant number: MT-5877.

*Correspondence to: Dr. Sebastian Haidarliu, Department of Neurobiology, The Weizmann Institute of Science, Rehovot 76100, Israel. Fax: 972-8-9346099. E-mail: sebastian.haidarliu@weizmann.ac.il

Ehud Ahissar holds the Helen Diller Family Professorial Chair of Neurobiology.

Received 11 September 2014; Revised 21 October 2014; Accepted 26 October 2014.

DOI 10.1002/ar.23102
Published online 18 November 2014 in Wiley Online Library (wileyonlinelibrary.com).

In whisking rodents, whisking and sniffing are described as motor strategies for gathering, respectively, tactile and olfactory information about the location, texture, and scent of objects (Deschênes et al., 2012). Sniffing is accompanied by synchronous repetitive protraction and retraction of the mystacial vibrissae and simultaneous oppositely phased rostrocaudal movements of the tip of the nose (Welker, 1964). Such movements are controlled by facial muscles that have been identified in many rodent species (Rinker, 1954; Klingener, 1964; Ryan, 1989). In rats, a part of these muscles is attached to the nasal cartilaginous skeleton (NCS) and mystacial pad (MP), and can move simultaneously both the vibrissae and the nose (Haidarliu et al., 2012).

For mice, a seemingly suitable scheme of muscle arrangement in the MP was proposed by Dörfl (1982) who grouped MP muscles into two categories, intrinsic and extrinsic. During the last three decades, this scheme was used as a template for defining facial muscle layout in studies performed in both mice and rats (Guntinas-Lichius et al., 2005; Angelov et al., 2007; Grosheva et al., 2008; Hill et al., 2008; Pavlov et al., 2008; Sinis et al., 2009). However, we consider that the four extrinsic muscles described by Dörfl (1982) cannot account for the diversity of movements of the vibrissae and MP. For instance, in the Dörfl's report, M. nasolabialis profundus, which participates in both translation of the MP and vibrissa movement, is missing. Wineski (1985) found that in hamsters, this muscle performs a forward pulling of the MP floor and that pars orbicularis oris of the M. buccinatorius, also not described in the Dörfl's study (1982), provokes the fanning of the ventral rows of vibrissae. Bosman et al. (2011) concluded that although the general structure of the MP in mice (Dörfl, 1982), hamsters (Wineski, 1985), and rats (Haidarliu et al., 2010) is similar, minor differences between species exist in the organization of the M. nasolabialis profundus.

Here, we used a histoenzymatic method to study the organization of striated muscles in the rostral part of the snout in mice. The origin and insertion sites of these muscles provide evidence for their potential role in whisking and nose movements.

## MATERIALS AND METHODS

### Animals

Our subjects were eight 2-week-old and 16 adult male C57BL/6 mice. The procedure for animal maintenance and all manipulations were approved by the Institute's Animal Care and Use Committee and conform to the NIH Principles of Laboratory Animal Care (Publication No. 86-23, revised 1985). Mice were anesthetized with urethane given intraperitoneally (25% (w/v); 0.65 mL/100 g body weight), perfused transcardially with 4% (w/v) paraformaldehyde and 5% (w/v) sucrose in 0.1 M phosphate buffer, pH 7.4, and their snouts were taken for histochemical study of the facial musculature.

### Visualization of Structural Organization of the Facial Musculature

Among the structural components of the vibrissa motor plant, vibrissa follicles are well distinguished among other tissue components even in unstained slices. Visualization of the other motor plant components, such as MP intrinsic collagenous structures and muscular network, requires special methods. Collagenous structures were visualized after histochemical staining or by their blue autofluorescence and the muscles by histoenzymatic reaction for cytochrome oxidase (CCO) activity.

Histoenzymatic staining for CCO activity was performed according to our modification (Haidarliu and Ahissar, 2001) of a procedure by Wong-Riley (1979). Briefly, after perfusion, MPs and the soft tissues of the rostral part of the snout were excised, placed between two pieces of stainless steel mesh into RCH-44 perforated plastic histology cassettes (Proscitech.com) to prevent tissue curling, and placed into 4% (w/v) paraformaldehyde solution with 30% (w/v) sucrose for postfixation. For the 2-week-old mice, postfixation was performed for entire rostral part of the snout, which was used for horizontal and coronal slicing. After 48 hr of postfixation, all tissue samples were sectioned into 30-μm-thick slices in the coronal, tangential, oblique, or horizontal planes using a sliding microtome (SM 2000R, Leica Instruments, Germany) coupled to a freezing unit (K400, Microm International, Germany). Free-floating slices were incubated in an oxygenated solution of 0.02% (w/v) cytochrome c (Sigma-Aldrich, St. Louis, MO), catalase (200 μg/mL), and 0.05 % (w/v) diaminobenzidine in 100 mM phosphate buffer at room temperature under constant agitation. When a clear differentiation between highly reactive and nonreactive tissue structures was observed, the incubation was arrested by adding 0.5 mL of 100 mM phosphate buffer into each of the incubation wells. Stained slices were washed, mounted on slides, cover-slipped with Entellan (Merck KGaA, Darmstadt, Germany), and examined by light microscopy. Striated muscles appeared stained dark brown.

### Visualization of the Cartilaginous and Collagenous Structures

Hyaline cartilages were visualized by staining the slices with alcian blue. Counterstaining with thiazine red was used to reveal collagenous structures and different cellular components in terms of the location of the red and blue fluorescence (Haidarliu et al., 2013). Briefly, after staining for CCO activity, the slices were mounted on slides, dried in the air, and stained for 30 min with 0.2% (w/v) alcian blue 8GX (Sigma-Aldrich) at room temperature. The slices were washed with distilled water, counterstained with 1% (w/v) thiazine red for 1 min at room temperature, and again washed with distilled water. Finally, they were dehydrated in sequential solutions of 50, 70, 95, and 100% (w/v) ethanol, cleared in xylene, and cover-slipped with Krystalon (Harleco, Lawrence, KS). The slices were examined using a Nikon Eclipse 50i microscope.

## RESULTS

### Musculature of the Mouse MP

***Intrinsic muscles.*** Intrinsic muscles were revealed in tangential slices obtained from slightly flattened MPs of adult mice and compared with homonymous muscles described previously in rats (Haidarliu et al., 2010). In both species, tangential slices contained entire sets of large mystacial vibrissae that are represented by four straddlers and five vibrissal rows (Fig. 1). Within the

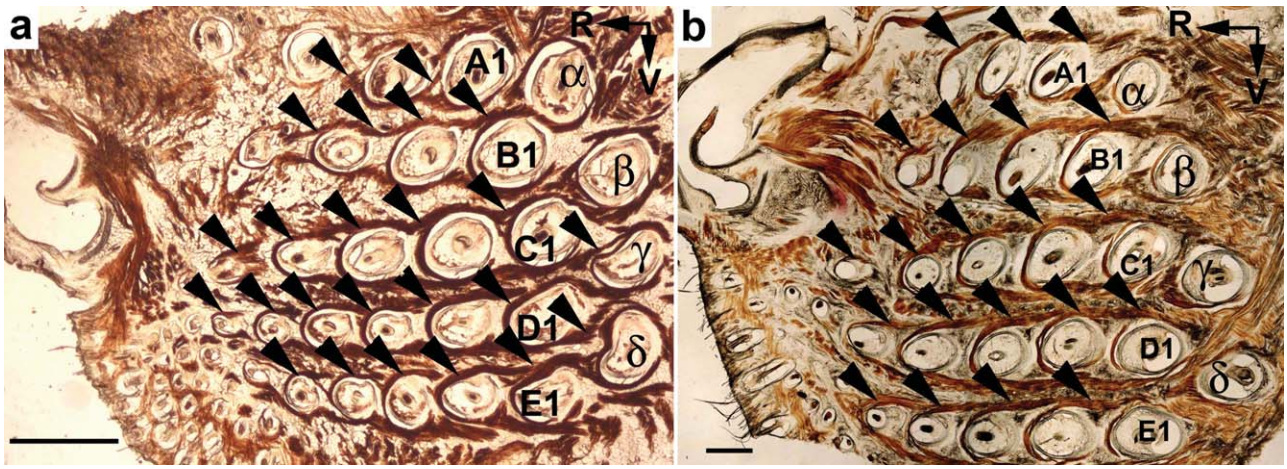


Fig. 1. Intrinsic muscles (indicated by arrow heads) in tangential slices of the MP of an adult mouse (**a**) and of an adult rat (**b**). The slices were stained for CCO activity. (α–δ), Straddler follicles; A1–E1, the first arc of vibrissa follicles arranged in rows; R, rostral; V, ventral. Scale bars = 1 mm.

rows, each pair of adjacent vibrissa follicles is interconnected by a sling-shaped intrinsic muscle. Each intrinsic muscle originates from the rostral surface at the proximal end of the rostrally located follicle, and is inserted into the distal end and adjacent corium of the caudally located follicle in both species. For the straddlers, the extremities of intrinsic muscles attach caudally to the corium. We confirm Dörfl's (1982) conclusion regarding similar organization of intrinsic muscles in mice and rats, though their dimensions in mice are about two times smaller than that in rats.

***Extrinsic muscles.*** Mouse MPs were cut in different planes with the aim of revealing extrinsic muscles together with their sites of attachment, that is, origins and insertion sites. All extrinsic muscles of the mouse MP were grouped according to the direction in which they move vibrissae, that is, (i) protractors, (ii) retractors, and (iii) vertical deflectors.

*Vibrissa protractors.* Extrinsic muscles that protract vibrissae are revealed in coronal, tangential, and oblique slices of the mouse snout. In coronal slices, a large symmetric muscle is seen fanning from medial to lateral (Fig. 2a). It consists of ventral and dorsal subdivisions. The dorsal subdivision originates from the rostral end of the premaxilla and is represented by pars media superior of the M. nasolabialis profundus. It extends dorsally, laterally, and caudally, and splits into three branches as it passes over partes maxillares superficialis et profunda of the M. nasolabialis profundus. These three branches are further directed toward the nasal compartment of the MP; they fan along the rows of vibrissa follicles and insert into the corium on both sides of the vibrissal rows A and B, forming fine rosette-like collagenous endings. The ventral subdivision known as pars media inferior of the M. nasolabialis profundus originates from the intermuscular septum and splits into four branches. Branches pass ventral and lateral to partes maxillares superficialis et profunda, encompass follicles of the vibrissal rows C, D, and E on both sides, and insert in the same fashion into the superficial layer (corium) of the maxillary compartment of the MP along the rows of vibrissa follicles. Between vibrissal rows B and C, two rows of muscle fascicles are attached to the corium: one relates to the pars media superior and the other to the pars media inferior (Fig. 2a,b).

In oblique slices of the rostral part of the snout, there are two muscles that can cause vibrissa protraction only in a part of the MP. These muscles originate from the lateral wall of the NCS, and are branches of M. nasolabialis profundus. One of them (pseudointrinsic slips) is directed dorsocaudally and inserts into the distal capsular ends of the vibrissa follicles and adjoining corium of the nasal compartment of the MP (features 11 and 13 in Fig. 2c–e). The other (posterior slips) is directed ventrocaudally (feature 12 in Fig. 2c) and inserts into the corium of the maxillary compartment of the MP.

*Vibrissa retractors.* In superficial tangential slices of the mouse MP, two large flat muscles enter the caudal part of the MP: M. nasolabialis, and M. maxillolabialis (features 1 and 2 in Fig. 3a). Terminal fibers of these muscles insert into the corium of the MP between the rows of vibrissae. Contraction of the analogous muscles in rats results in vibrissa retraction, which occurs during the third phase of the whisking cycle (Hill et al., 2008).

In oblique tangential slices of the mouse MP, partes maxillares superficialis et profunda and pars interna profunda of the M. nasolabialis profundus appear as flat bipennate muscles that originate from the lateral wall of the NCS (features 4 to 6 in Fig. 3b). These muscles fan and reach the caudal part of the MP, where they insert into the subcapsular fibrous mat under rows A and B (pars interna profunda) and under rows C–E (partes maxillares superficialis et profunda) of vibrissa follicles. Transversally cut partes maxillares are also seen in coronal slices (features 2 and 3 in Fig. 2a). Contraction of the pars interna profunda and of the partes maxillares superficialis et profunda of the M. nasolabialis profundus pulls the subcapsular fibrous mat rostrally, together with the proximal ends of vibrissa follicles, and causes retraction of the vibrissae, as described in rats (Deschênes et al., in press).

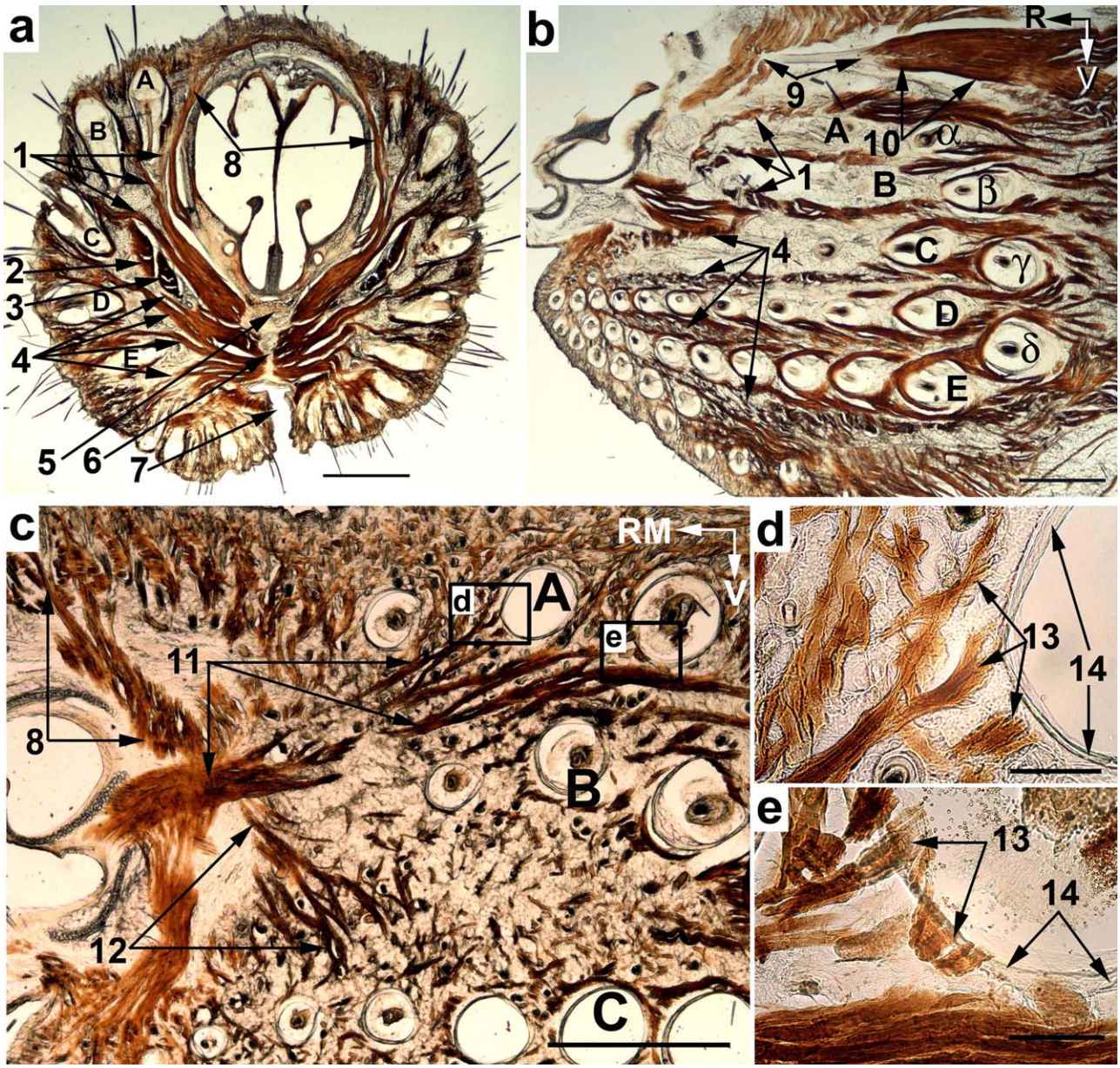


Fig. 2. Extrinsic vibrissa protracting muscles. Light microscopy of a coronal (**a**) and a tangential (**b** and **c**) slices of the snout of adult mice. Slices were stained for CCO activity. (**d**, **e**) Enlarged boxed areas in (**c**). All marked muscle parts/fascicles belong to the M. nasolabialis profundus. (α–δ), Straddle follicles; A–E, rows of vibrissa follicles. (1) Three muscle fascicles of the pars media superior; (2) pars maxillaris superficialis; (3) pars maxillaris profunda; (4) four muscle fascicles of the pars media inferior; (5) premaxilla; (6) septum intermusculare; (7) philtrum; (8) the most superficial slip of the pars interna; (9) tendon and (10) belly of the M. dilator nasi; (11) pseudointrinsic, and (12) posterior slips of the pars interna; (13) insertion sites of the pseudointrinsic slips; (14) capsules of the vibrissa follicles. R, rostral; RM, rostromedial; V, ventral. Scale bars = 1 mm (a, b, c) and 0.1 mm (d, e).

*Vertical vibrissa deflectors.* In the ventral part of the mouse MP, muscle fascicles representing pars orbicularis oris of the M. buccinatorius are seen approaching and entering the ventral part of the maxillary compartment of the MP (feature 3 in Fig. 3a). This muscle originates from the skin of the lower lip and from the muscle fibers of the M. buccinatorius. Muscle fascicles are directed from ventrocaudal to dorsorostral and insert into the corium of the maxillary compartment of the MP at the level of the arcs 2–6 of the vibrissa follicles. Contraction of this muscle pulls the distal ends of the follicles of the maxillary compartment of the MP, causing ventrocaudal deflection of the vibrissae and an increase in the vertical spread of the vibrissae.

M. transversus nasi is composed of a number of muscle fascicles that originate from the dorsal nasal aponeurosis, as well as from the myomyous fiber junctions along the midline (Fig. 4). Terminal fibers of this muscle insert into the corium of the nasal compartments of the MP bilaterally. Contraction of M. transversus nasi pulls the corium

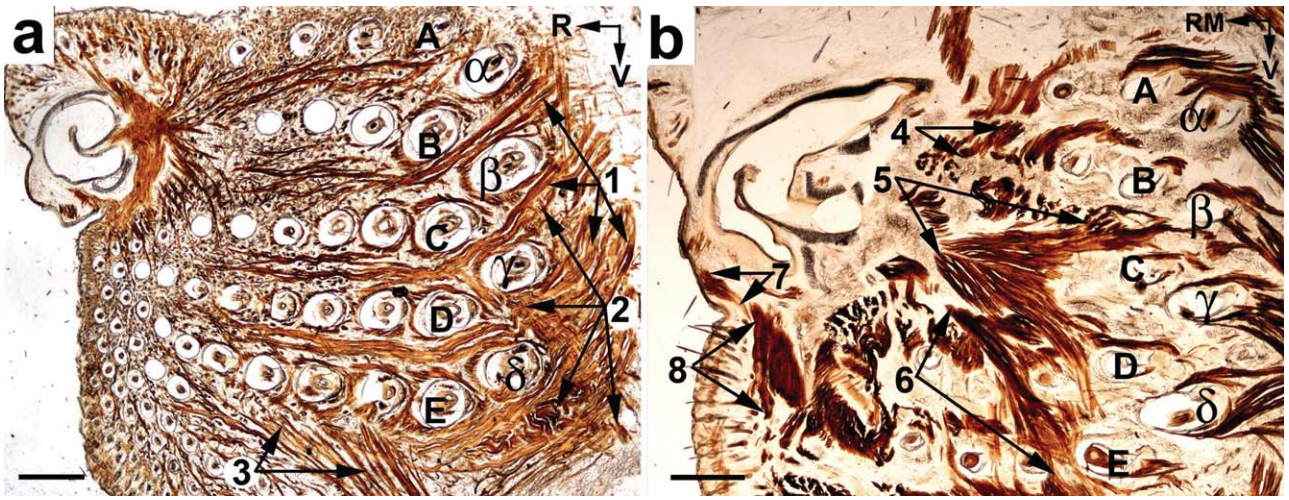


Fig. 3. Extrinsic vibrissa retracting muscles. A superficial tangential (**a**) and a deep oblique (**b**) slice of the MP of adult mice. The slices were stained for CCO activity. (1) M. nasolabialis; (2) M. maxillolabialis; (3) pars orbicularis oris of the M. buccinatorius; (4–6) partes interna profunda, maxillaris superficialis, et maxillaris profunda, respectively, of the M. nasolabialis profundus; (7) M. depressor rhinarii; (8) M. depressor septi nasi. (α–δ), Straddler follicles; A–E, rows of vibrissa follicles; R, rostral; RM, rostromedial; V, ventral. Scale bars = 1 mm.

of the nasal compartment of the MP and the distal ends of the vibrissa follicles in the dorsomedial direction, causing dorsal deflection and increased vertical spread of the vibrissae. Contraction of the rostral-most fascicles of this muscle can also pull rhinarium dorsally.

## Musculature Providing Rhinarial Motion

Muscles that move rhinarium in mice belong to the rhinarial motor plant and are similar to those described in rats (Haidarliu et al., 2013). These muscles can be divided into three groups: (i) muscles attached to the rhinarium proper; (ii) muscles that move rhinarium by moving NCS; and (iii) muscles that move rhinarium by pulling dorsum nasi. Muscles of the first group are attached directly to the rhinarium, whereas muscles of the other two groups are connected to nonmuscular structures that mediate muscle effect on the rhinarium. These structures have sliding connections with the skull. To clarify the mechanisms by which muscle contraction moves the rhinarium, we examined the anatomical relationships among the muscles, the nonmuscular intermediate structures, and rhinarium.

The tip of the nose (rhinarium) and vibrissae are the most prominent motile elements of the snout. In the rhinarium, we observed an internarial area that is represented by two symmetric narial pads (feature 1 in Fig. 5a). In mice, the narial pads are approximately two times smaller

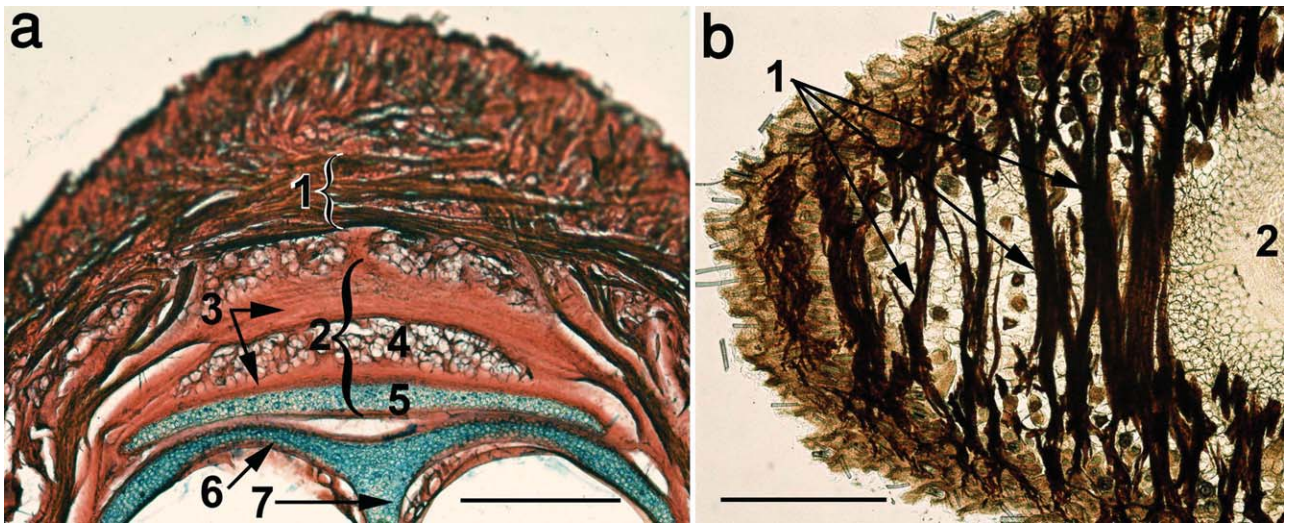


Fig. 4. Light microscopy of a coronal slice of the snout of an adult (**a**) and of a horizontal slice of a 2-week-old (**b**) mouse. Both slices were stained for CCO activity, coronal slice being supplementary stained with alcian blue and thiazine red. (1) M. transversus nasi; (2) DNC; (3) fibrous compartment of the DNC; (4) fatty pad; (5) hyaline compartment of the DNC; (6) nasal tectum; (7) septum. Scale bars = 0.5 mm.

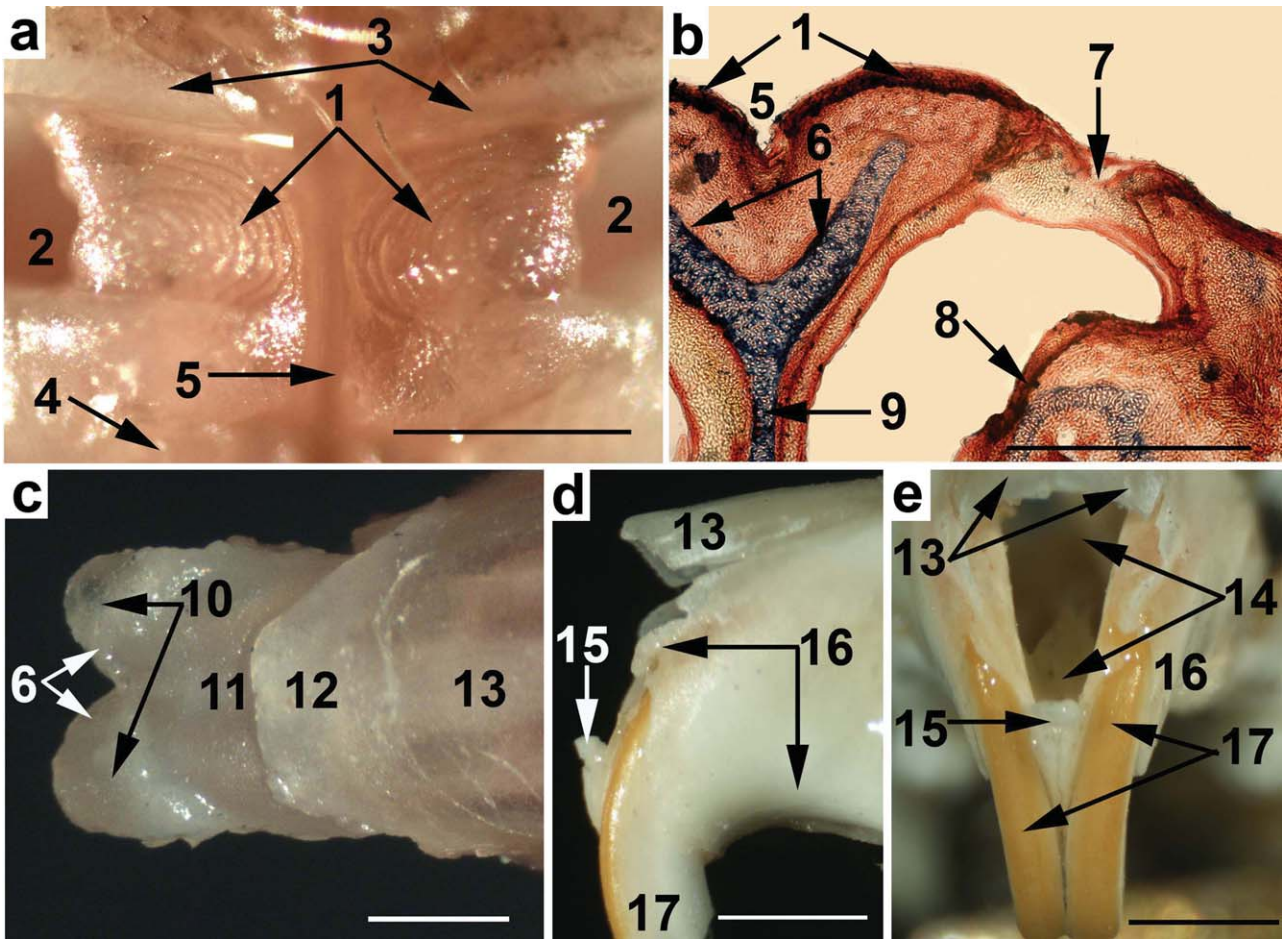


Fig. 5. Morphology of the rostral part of the nose in mice. (**a**) A photograph of the rhinarium of an adult mouse; (**b**) Light microscopy of a horizontal slice of the snout of a 2-week-old mouse; (**c**) A photograph of the dissected NCS of an adult mouse; (**d**) Lateral and (**e**) frontal views of the skull of an adult mouse. (1) Narial pads; (2) nostrils; (3) dorsal, and (4) ventral integumental folds; (5) median sulcus; (6) lateral ventral processes of the NCS; (7) ventral edge of the nostril; (8) atrioturbinate; (9) septum; (10) cupular cartilage; (11) nasal tectum; (12) dorsal nasal cartilage; (13) nasal bones; (14) pyriform aperture; (15) rostral spine of the premaxilla (16); (17) incisives. Scale bars = 1 mm.

than those in rats (Haidarliu et al., 2013). They are characterized by the presence of rhinoglyphics of about the same size as that in rats (Fig. 5a). In horizontal slices of the rhinarium, the narial pads are tightly connected to the lateral ventral processes of the NCS (features 1 and 6 in Fig. 5b). Dissected NCS maintains its integrity (Fig. 5c) and has an appearance and mobility similar to the respective structures in rats (Haidarliu et al., 2013).

The NCS is attached to the skull at its caudal end. At the level of the pyriform aperture, NCS forms a telescopic connection with the nasal bones and premaxilla. This connection allows a sliding movement of the NCS relative to the skull parallel to its rostrocaudal axis, as well as turning of the rostral end of the NCS in the dorsoventral and lateral directions. Rostral edges of the premaxilla, which fringe the pyriform aperture, are tilted laterally, forming an opening reminiscent of a funnel that may facilitate turning of the entire NCS in different directions (Fig. 5d,e).

Dorsal surface of the caudal half of the NCS is covered by the dorsal nasal cartilage (DNC) that is attached to the nasal bones (features 12 and 13 in Fig. 5c). The DNC is composed of hyaline and fibrous compartments, as in rats (Haidarliu et al., 2013). However, in mice, within the fibrous compartment of the DNC, a flat wide fatty pad is present (feature 4 in Fig. 4a, and feature 7 throughout panels in Fig. 6). Interior structural features of the pad were visualized by staining the collagenous meshwork (Fig. 6a,b,f). The pad has spongious architecture with irregular spaces filled with adipocytes containing large lipid droplets. Such a soft structure may provide protection of the underlying nasal structures from injury as the mouse explores objects with its nose.

In both NCS and DNC, hyaline has a similar appearance: it intensively stains with alcian blue (Fig. 6a–d) and possesses a strong autofluorescence (Fig. 6e). However, in the NCS, a columnar arrangement of chondrocytes is clearly observable (feature 8 in Fig. 6c), whereas in the ventral compartment of the DNC, such an arrangement is not discernable (Fig. 6d). Yet, the apparent lack of chondrocyte clusters in the DNC could be a consequence of their deformation during nose movements.

***Muscles attached to the rhinarium.*** Two rhinarial muscles, Mm. levator et depressor rhinarii, directly

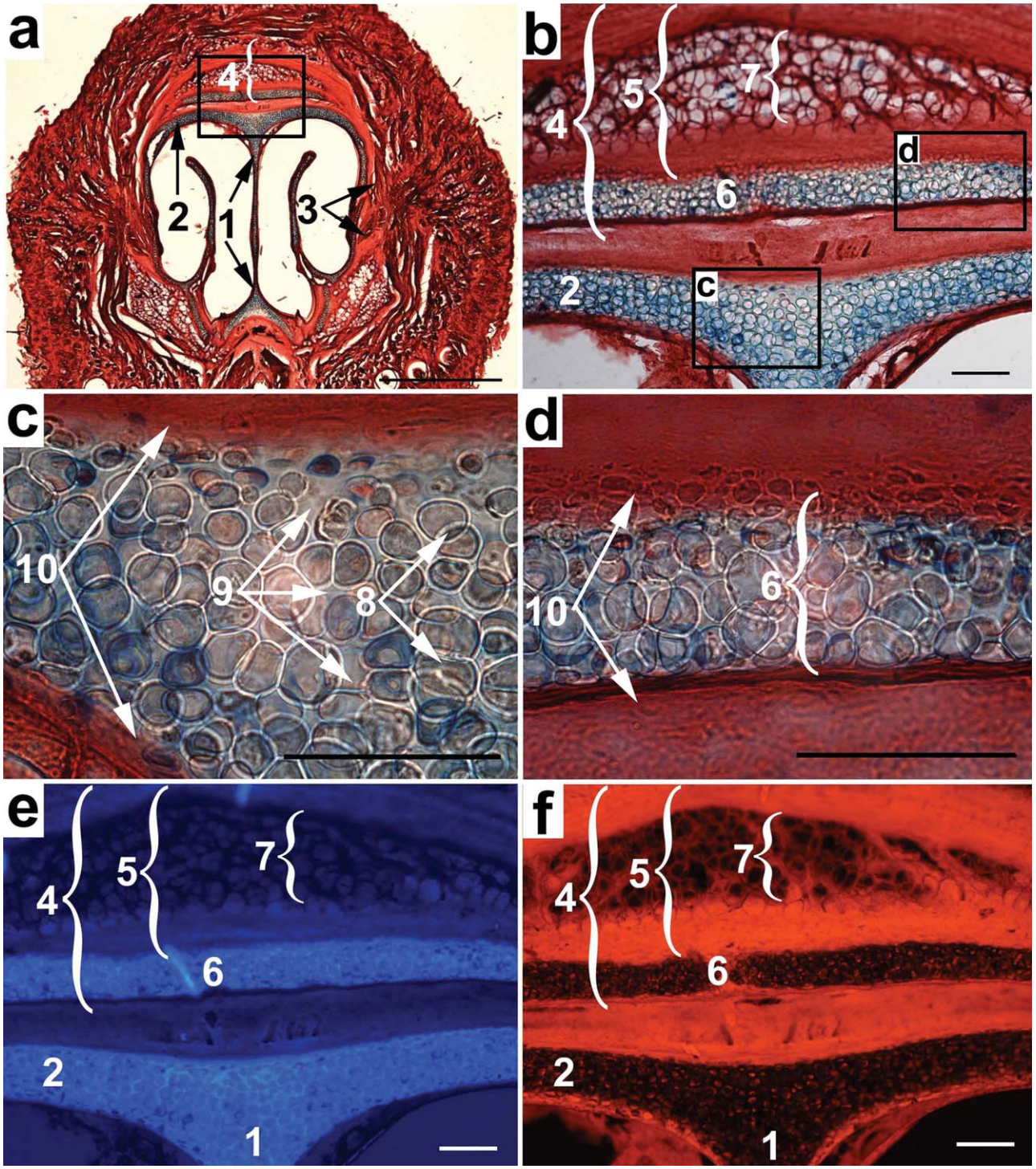


Fig. 6. Light microscopy (**a–d**), autofluorescence (**e**), and thiazine red fluorescence (**f**) in a coronal slice cut from the rostral part of the snout of an adult mouse. The slice was stained for CCO reactivity supplemented with thiazine red and alcian blue. (b, e, f) Enlarged boxed area in (a). Panels (c) and (d) represent respectively marked and enlarged boxed areas in (b). (1) Septum; (2) roof cartilage; (3) muscle attachments to the lateral wall of the NCS; (4) DNC; (5) dorsal and (6) ventral compartments of the DNC; (7) fatty pad; (8) chondrocyte clusters; (9) matrix; (10) perichondrium. Scale bars = 1 mm (a) and 0.1 mm (b–f).

attach to the rhinarium. M. levator rhinarii originates from the dorsal integumental fold and inserts into the skin of the dorsum nasi (feature 1 in Fig. 7). M. depressor rhinarii originates from the ventral integumental fold and inserts into the upper lip (feature 7 in Fig. 3b). The function of these two muscles may be similar in

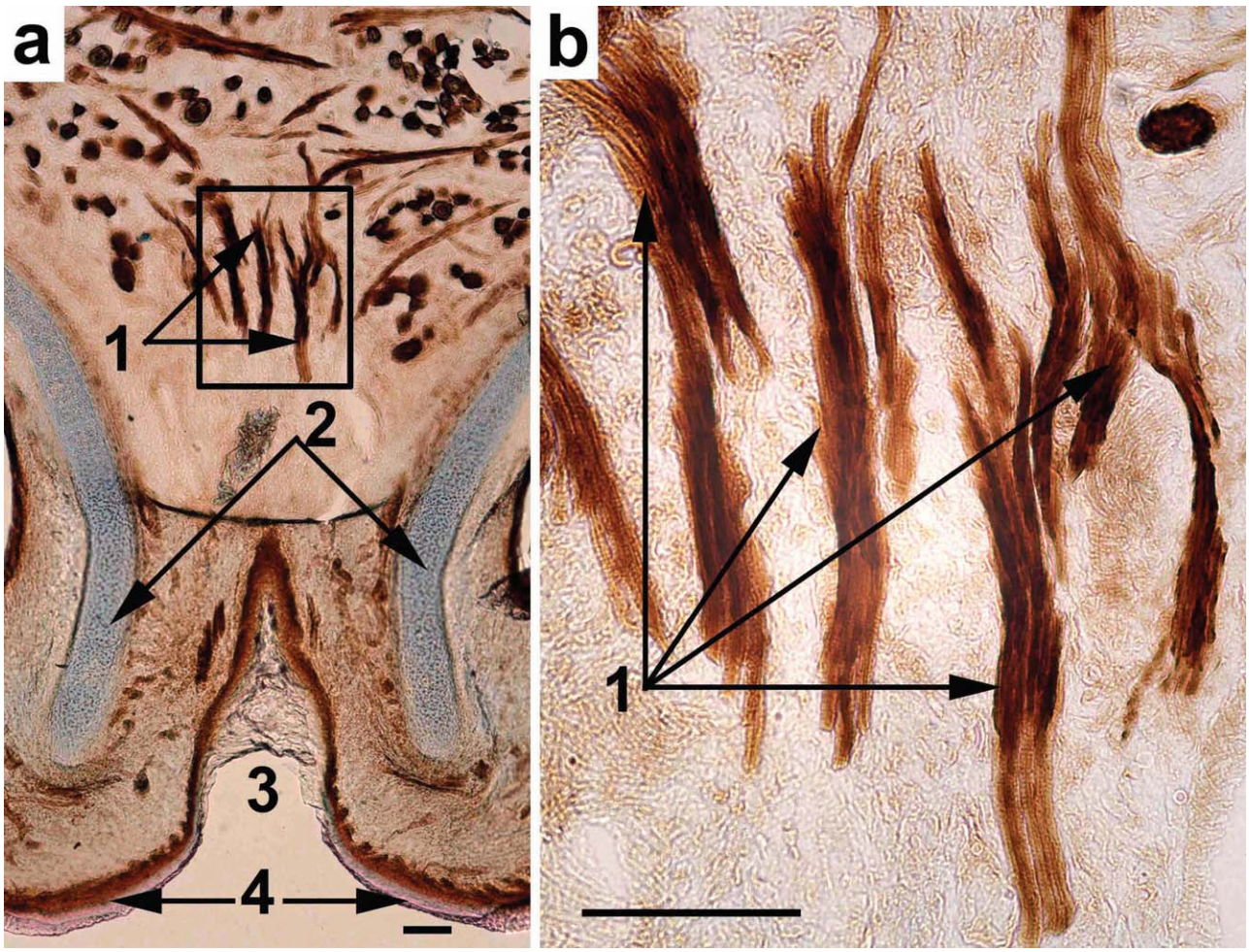


Fig. 7. Light microscopy of a coronal slice of the rostral end of the mouse snout. (**b**) Enlarged boxed area in (**a**). The slice was stained for CCO activity supplemented with alcian blue and thiazine red. (1) M. levator rhinarii; (2) lateral ventral processes of the NCS; (3) median sulcus; (4) narial pads (ventral edges). Scale bars = 0.1 mm.

both mice and rats: they may stretch integumental folds, stabilize the rhinarium (narial pads) during object touch, and deflect the rhinarium vertically (Haidarliu et al., 2013).

***Muscles that move rhinarium by moving the NCS.*** These muscles are represented by separate parts/slips of the M. nasolabialis profundus. They were already mentioned earlier: the posterior and pseudointrinsic slips of the pars interna in Fig. 2c and pars interna profunda and partes maxillares superficialis et profunda in Fig. 3b. These muscles originate from the lateral wall of the NCS (feature 3 in Fig. 6a); thus, the effects of their contraction on the rhinarium are mediated by the NCS and could be described as rhinarium retraction.

M. depressor septi nasi originates from the rostroventral edge of the nasal septum, rostral to the anterior transverse lamina of the NCS, and inserts into the upper lip (feature 8 in Fig. 3b). Contraction of this muscle will cause ventral deflection of the rostral end of the NCS and of the rhinarium.

***Muscles that move rhinarium by affecting dorsum nasi.*** At the dorsal edge of the MP, one can see M. dilator nasi (features 9 and 10 in Fig. 2b). It originates from the ventral margin of the orbit. The belly of this muscle is fleshy, has a bipennate structure, and extends rostrally, up to the level of the second arc of the mystacial vibrissa follicles. The tendon runs rostralward and inserts into the aponeurosis above the movable nasal cartilages.

Rostral-most fascicles of the M. transversus nasi may reach the tip of the nose, where they insert into the corium close to the dorsolateral part of the rhinarium (feature 1 in Fig. 4b). Contraction of the rostral part of the M. transversus nasi will pull the rhinarium in a dorsal direction.

Finally, according to Rinker (1954), the most superficial slip of the pars interna of the M. nasolabialis profundus in many rodents originates from the lateral wall of the nasal cartilage and passes onto the bridge of the nose at a location superficial to the tendon of M. dilator nasi. We observed that some fascicles of this slip turn rostrally, encircling the cupula nasi, and insert into the

**TABLE 1. Characteristics of individual muscles of the vibrissal and rhinarial motor plants**

| Muscle name and illustrating figure | Origin | Insertion site | Effect on vibrissa | Effect on rhinarium |
|---|---|---|---|---|
| Buccinatorius, pars orbicularis oris; Fig. 3a | Skin of the lower lip | Corium of the maxillary compartment | Ventral deflection, increased vertical spread in the maxillary compartment | No effect |
| Dilator nasi; Fig. 2b | Ventral orbit, zygomatic notch | Aponeurosis above nasal cartilages | No effect | Retraction, dorsal or lateral deflection |
| Maxillolabialis; Fig. 3a | Maxilla | Corium of the entire MP | Retraction in the entire MP | No effect |
| Nasolabialis; Fig. 3a | Nasal bone | Corium of the entire MP | Retraction in the entire MP | No effect |
| Transversus nasi[a]; Fig. 4a,b | Dorsal nasal aponeurosis, myomyous junctions | Corium of the nasal compartment | Dorsal deflection, increased vertical spread in the nasal compartment | Dorsal deflection |
| Nasolabialis profundus, pars interna profunda[a]; Fig. 4b | Nasal cartilage | Deep fibrous mat of the nasal compartment | Retraction in the nasal compartment | Retraction |
| Pars interna, posterior slips[a]; Fig. 2c | Nasal cartilage | Corium, maxillary compartment | Protraction in the maxillary compartment | Retraction |
| Pars interna, pseudointrinsic slips[a]; Fig. 2c–e | Nasal cartilage | Follicles in the rows A and B, corium | Protraction in the nasal compartment | Retraction |
| Pars interna, superficial slips; Fig. 2a–c | Nasal cartilage | Corium of the dorsum nasi | No effect | Dorsal deflection |
| Pars maxillaris profunda[a]; Figs. 2a and 3b | Nasal cartilage | Deep fibrous mat of the maxillary compartment | Retraction in the maxillary compartment | Retraction |
| Pars maxillaris superficialis[a]; Figs. 2a and 3b | Nasal cartilage | Deep fibrous mat of the maxillary compartment | Retraction in the maxillary compartment | Retraction |
| Pars media inferior; Fig. 2a,b | Intermuscular septum | Corium of the maxillary compartment | Protraction in the maxillary compartment | No effect |
| Pars media superior; Fig. 2a,b | Premaxilla, rostral end | Corium, nasal compartment | Protraction in the nasal compartment | No effect |
| Intrinsic muscles of the mystacial pad; Fig. 1a | Follicular capsules, proximal ends | Distal ends of follicular capsules, corium | Protraction in the entire mystacial pad | No effect |
| Levator rhinarii; Fig. 7a,b | Rhinarium | Corium of the dorsum nasi | No effect | Dorsal deflection |
| Depressor rhinarii; Fig. 3b | Rhinarium | Corium of the upper lip | No effect | Ventral deflection |
| Depressor septi nasi; Fig. 3b | Septum nasi, ventral edge | Corium of the upper lip | No effect | Ventral deflection |

[a]Muscles involved in both vibrissal and rhinarial motor plants.

corium of the dorsum nasi above the rhinarium (feature 8 in Fig. 2a,c). We suggest that contraction of these muscle fascicles can cause a slight dorsiflection of the rhinarium.

Table 1 summarizes the above-described extrinsic muscles and those involved in controlling the rhinarium and MP, together with expected effects of their contraction.

## DISCUSSION

### Extrinsic Muscles of the Mouse MP

In Dörfl's (1982) scheme of muscle arrangement in the mouse MP, vibrissa protraction can be driven by contraction of the intrinsic muscles and of only one extrinsic vibrissal muscle (M. nasalis). According to the analysis of Diogo et al. (2009) in an exhaustive literature review of comparative anatomical data, M. nasalis was described only in anthropoids and humans. In rodents, M. nasalis was not defined, but rodents may have analogous muscles, such as M. maxillolabialis and M. nasolabialis profundus (Ryan, 1989; Diogo, 2009). A comparison of the descriptions and illustrations of the snout musculature provided for mice by Dörfl (1982) with those by Rinker (1954), Klingener (1964), and Ryan (1989) for different rodents, Wineski (1985) for hamster, and our findings for rats (Haidarliu et al., 2010) and mice (this study), leads to the conclusion that Dörfl's (1982) M. nasalis corresponds to partes mediae superior et inferior of the M. nasolabialis profundus (Fig. 2). However, Dörfl's (1982) M. nasalis does not represent the entire partes mediae because it contains only five muscle slips out of the seven that are described in this study (pars media superior is composed of three muscle slips and pars media inferior is of four similar slips).

According to Diogo et al. (2009), it is important to maintain the stability of the anatomical nomenclature that has been largely used in thousands of publications during many decades. Yet Dörfl's (1982) attempt to describe an apparently new extrinsic vibrissa protracting muscle in mice under the name M. nasalis is improper, because this new muscle does not exist as a separate muscular unit because it contains only fragments of the two already known parts of the M. nasolabialis profundus.

In this study, we describe four extrinsic vibrissa protractors that belong to the M. nasolabialis profundus: partes mediae superior et inferior and posterior and pseudointrinsic muscular slips of the pars media. Vibrissa retraction is provided by five different extrinsic muscles: two of them are separate muscles, that is, M. nasolabialis and M. maxillolabialis, which pull the distal ends of vibrissa follicles caudalward. These two muscles were described in several studies of facial muscles in different mammals (Rinker, 1954; Klingener, 1964; Ryan, 1989; Grant et al., 2013), including whisking species such as mice (Dörfl, 1982), hamsters (Wineski, 1985), and rats (Berg and Kleinfeld, 2003; Hill et al., 2008; Haidarliu et al., 2010). The other three muscles belong to M. nasolabialis profundus, that is, partes maxillares superficialis et profunda and pars interna profunda, which pull the proximal ends of vibrissa follicles rostralward. We thus suggest that the name M. nasalis should be dropped, and the anatomical nomenclature updated to M. nasolabialis profundus, whose contraction produces forward translation of the MP through protraction of partes mediae superior et inferior.

Multiple vibrissa protractors and retractors, together with vertical vibrissa deflectors, may be important in executing complex whisker movements. In particular, asynchronous and multidirectional vibrissa movements can be explained partially by the involvement of the accessory vibrissa protractors, such as the posterior and pseudointrinsic slips of the pars interna of the M. nasolabialis profundus and the vertical vibrissa deflectors, such as M. transversus nasi and pars orbicularis oris of the M. buccinatorius. These muscles may be important in providing whisking synchrony during bilateral location comparisons (Ahissar and Knutsen, 2008; Knutsen and Ahissar, 2009; Horev et al., 2011), as well as morphological coding (Bagdasarian et al., 2013). Excitatory and inhibitory interactions between the brainstem trigeminal neurons and facial nucleus motoneurons may cause asynchronous movement of the neighboring vibrissa (Erzurumlu and Killackey, 1979; Kleinfeld et al., 1999; Sachdev et al., 2002; Brecht et al., 2006; Deutsch et al., 2012; Sherman et al., 2013).

## Snout Structures Involved in Active Touch by Rhinarium

In rats, rhinarium is considered important in touch perception because of its dense innervation (Silverman et al., 1986) and high motility. In mice, like in rats, rhinarium is easily movable and possesses only two muscles: Mm. depressor et levator rhinarii. These muscles are small and can only moderately stretch integumental folds in the vertical direction, stabilize the position of the rhinarium during object touch, and slightly move it in dorsoventral direction.

In mice and rats, the rhinarium is tightly attached to the nasal cartilages, and its movement is determined by the movement of the rostral end of the NCS. In our recent study in rats (Haidarliu et al., 2013), we described morphology and function of the cartilaginous complex that includes the NCS and the DNC and suggested that similar structures may exist in other rodents as well. In this study, we confirmed that mice's NCS is also attached to the skull by a telescopic connection. This allows the NCS to move relative to the skull along its rostrocaudal axis and to deflect the rostral end in lateral, dorsal, and ventral directions. Telescopic connections that make the nose movable were already described in Eurasian common shrews and in water shrews by Maier (2002). However, in shrews, such connections were found only between cartilages, whereas in mice, between cartilages and the bones of the skull. Another difference refers to the muscles: in shrews, nose retraction is provided by the M. retractor proboscides (Maier, 2002), whereas in mice, by the Mm. dilator nasi and nasolabialis profundus.

In mice and rats, the DNC overlies the caudal half of the NCS. We suggest that in these species the DNC limits bending of the NCS, returning it to the resting position after deflection, as well as protecting vulnerable intranasal structures from mechanical impacts. Like in rats, the DNC in mice contains hyaline and fibrous compartments. However, in mice, the fibrous compartment of the DNC contains an additional structure, consisting of a spongy meshwork of thin interlacing collagen fibers (fatty pad) encased into the dorsal fibrous compartment of the DNC (Figs. 4 and 6). Fatty pad contains adipocytes surrounded by collagen shells. We suggest that the function of such resilient fatty pad consists in providing mechanical protection for the tender structures of the nose from injury.

Most parts/slips of the M. nasolabialis profundus take origin on the lateral wall of the NCS (Fig. 6a) and insert into the corium or in the subcapsular fibrous mat of the MP, where they spread forming rosette-like attachment points. This arrangement increases the surface of muscle attachment, and provides an even distribution of force in the corium during muscle contraction. When both deep, that is, partes maxillares superficialis et profunda, and pars interna profunda, and superficial, that is, partes mediae superior et inferior, subdivisions of the M. nasolabialis profundus contract simultaneously, they pull the corium and the deep fibrous mat of the MP rostralward, provoking ensemble protraction of the vibrissae. At the same time, the NCS moves in the caudal direction, provoking nose retraction. This sequence of movements occurs during the inspiratory phase of the sniffing behavior as described by Welker (1964), O'Connor et al. (2010), Deschênes et al. (2012), and Moore et al. (2013).

In both rats and mice, M. dilator nasi has similar configuration and attachment sites. We suggest that the function of M. dilator nasi in mice is also similar to that of the homonymous muscle in rats (Deschênes et al., in press), that is, unilateral contraction lifts the nose and deflects it sideway toward the side of contraction. Bilateral contraction of the M. dilator nasi will lead to dorsiflection of the tip of the nose. Rostral fascicles of the M. transversus nasi also can cause dorsal deflection of the nose (Table 1). The apparent protraction of the nose results from elastic forces that restore the rostral position of the NCS as the muscles relax.

## CONCLUSIONS

1. The organization of the rostral facial musculature in mice is similar to that in rats.
2. The muscles are attached to the touch-sensitive structures of the snout by means of cartilaginous and collagenous structures that mediate active touch by the rhinarium and vibrissae, respectively.
3. In mice, the DNC contains a spongious fatty pad made of collagenous fibers with incased adipocytes. This fatty pad seems to function as a shock absorber.
4. The term M. nasalis is currently used to designate a vibrissa protracting extrinsic muscle in the snout of mice and rats. In fact, this muscle only partially corresponds to two already known vibrissa protractors (partes mediae superior et inferior of the M. nasolabialis profundus). Thus, the term M. nasalis is inappropriate to describe the complexity of snout muscles in rodents.
5. Partes mediae superior et inferior of the M. nasolabialis profundus may be considered as the main extrinsic vibrissa protractors. The other two extrinsic vibrissa protractors (pseudointrinsic and posterior slips of the pars interna of the M. nasolabialis profundus) can be considered as accessory vibrissa protractors.

## LITERATURE CITED


Ahissar E, Arieli A. 2001. Figuring space by time. Neuron 32:185–201.

Ahissar E, Knutsen PM. 2008. Object localization with whiskers. Biol Cybern 98:449–458.

Angelov DN, Ceynowa M, Guntinas-Lichius O, Streppel M, Grosheva M, Kiryakova SI, Maegele E, Irintchev AP, Neiss WF, Sinis N, Alvanou A, Dunlop SA. 2007. Mechanical stimulation of paralyzed vibrissal muscles following facial nerve injury in adult rat promotes full recovery of whisking. Neurobiol Dis 26:229–242.

Bagdasarian K, Szwed M, Knutsen PM, Deutsch D, Derdikman D, Pietr M, Simony E, Ahissar E. 2013. Pre-neuronal morphological processing of object location by individual whiskers. Nat Neurosci 16:622–631.

Bahar A, Dudai Y, Ahissar E. 2004. Neural signature of taste familiarity in the gustatory cortex of the freely behaving rat. J Neurophysiol 92:3298–3308.

Berg RW, Kleinfeld D. 2003. Rhythmic whisking by rat: retraction as well as protraction of the vibrissae is under active muscular control. J Neurophysiol 89:104–117.

Bosman LWJ, Houweiling AR, Owens CB, Tanke N, Shevchouk OT, Rahmati N, Teunissen WHT, Ju C, Gong W, Koekkoek SKE, De Zeeuw CI. 2011. Anatomical pathways involved in generating and sensing rhythmic whisker movements. Front Integr Neurosci 5: 53. doi: 10.3389/fnint.2011.00053.

Brecht M, Grinevich V, Jin T-E, Margie T, Osten P. 2006. Cellular mechanisms of motor control in the vibrissal system. Eur J Physiol 453:269–281.

Deschênes M, Moore JD, Kleinfeld D. 2012. Sniffing and whisking in rodents. Curr Opin Neurobiol 22:243–250.

Deschênes M, Haidarliu S, Demers M, Moore J, Kleinfeld D, Ahissar E. Muscles involved in naris dilation and nose motion in rat. Anat Rec, in press.

Deutsch D, Pietr M, Knutsen PM, Ahissar E, Schneidman E. 2012. Fast feedback in active sensing: touch-induced changes to whisker-object interaction. PLoS ONE 7:e44272.

Diogo R. 2009. The head and neck muscles of the Philippine colugo (Dermoptera: *Cynocephalus volans*), with a comparison to treeshrews, primates, and other mammals. J Morphol 270:14–51.

Diogo R, Wood BA, Aziz MA, Rurrows A. 2009. On the origin, homologies and evolution of primate facial muscles, with a particular focus on hominoids and a suggested unifying nomenclature for the facial muscles of the Mammalia. J Anat 215:300–319.

Dörfl J. 1982. The musculature of the mystacial vibrissae of the white mouse. J Anat 135:147–154.

Erzurumlu RS, Killackey HP. 1979. Efferent connections of the brainstem trigeminal complex with the facial nucleus in the rat. J Comp Neurol 188:75–86.

Grant RA, Haidarliu S, Kennerley NJ, Prescott TJ. 2013. The evolution of active vibrissal sensing in mammals: evidence from vibrissal musculature and function in the marsupial opossum *Monodelphis domestica*. J Exp Biol 216:3483–3494.

Grill HJ, Norgren R. 1978. The taste reactivity test. I. Mimetic responses to gustatory stimuli in neurologically normal rats. Brain Res 143:263–279.

Grosheva M, Guntinas-Lichius O, Angelova SK, Kuerten S, Alvanou A, Streppel M, Skouras E, Sinis N, Pavlov S, Angelov DN. 2008. Local stabilization of microtubule assembly improves recovery of facial nerve function after repair. Exp Neurol 209: 131–144.

Guntinas-Lichius O, Irintchev A, Streppel M, Lenzen M, Grosheva M, Wewetzer K, Neiss WF, Angelov DN. 2005. Factors limiting motor recovery after facial nerve transection in the rat: combined structural and functional analyses. Eur J Neurosci 21:391–402.

Haidarliu S, Ahissar E. 2001. Size gradients of barreloids in the rat thalamus. J Comp Neurol 429:372–387.

Haidarliu S, Simony E, Golomb D, Ahissar E. 2010. Muscle architecture in the mystacial pad of the rat. Anat Rec 293:1192–1206.

Haidarliu S, Golomb D, Kleinfeld D, Ahissar E. 2012. Dorsorostral snout muscles in the rat subserve coordinated movement for whisking and sniffing. Anat Rec 295:1181–1191.

Haidarliu S, Kleinfeld D, Ahissar E. 2013. Mediation of muscular control of rhinarial motility in rats by the nasal cartilaginous skeleton. Anat Rec 296:1821–1832.

Hill DN, Bermejo R, Zeigler HP, Kleinfeld D. 2008. Biomechanics of the vibrissa motor plant in rat: rhythmic whisking consists of triphasic neuromuscular activity. J Neurosci 28:3438–3455.

Horev G, Saig A, Knutsen PM, Pietr M, Yu C, Ahissar E. 2011. Motor-sensory convergence in object localization: a comparative study in rats and humans. Phil Trans R Soc B 366:3070–3076.

Katz DB, Simon SA, Nicolelis MAL. 2001. Dynamic and multimodal responses of gustatory cortical neurons in awake rats. J Neurosci 21:4478–4489.

Kepecs A, Uchida N, Mainen ZF. 2006. The sniff as a unit of olfactory processing. Chem Senses 31:167–179.

Kleinfeld D, Ahissar E, Diamond ME. 2006. Active sensation: insights from the rodent vibrissa sensorimotor system. Curr Opin Neurobiol 16:435–444.

Kleinfeld D, Berg RW, O'Connor SM. 1999. Anatomical loops and their electrical dynamics in relation to whisking by rat. Somatosens Mot Res 16:69–88.

Klingener D. 1964. The comparative myology of four dipodoid rodents (Genera Zapus, Napeozapus, Sicista, and Jaculus). Misc Publ Mus Zool Univ Mich 124:1–100.

Knutsen PM, Ahissar E. 2009. Orthogonal coding of object location. Trends Neurosci 32:101–109.

Maier W. 2002. Zur functionellen Morphologie der rostralen Nasenknorpel bei Soriciden. Mamm Biol 67:1–17.

Maravall M, Diamond ME. 2014. Algorithms of whisker-mediated touch perception. Curr Opin Neurobiol 25:176–186.

Mitchinson B, Grant RA, Arkley K, Rankov V, Perkon I, Prescott TJ. 2011. Active vibrissal sensing in rodents and marsupials. Phil Trans R Soc B 366:3037–3048.

Moore JD, Deschênes M, Furuta T, Huber D, Smear MC, Demers M, Kleinfeld D. 2013. Hierarchy of orofacial rhythms revealed through whisking and breathing. Nature 497:205–210.

O'Connor DH, Clack NG, Huber D, Komiyama T, Myers EW, Svoboda K. 2010. Vibrissa-based object localization in head-fixed mice. J Neurosci 30:1947–1967.

Pavlov SP, Grosheva M, Streppel M, Guntinas-Lichius O, Irintchev A, Skouras E, Angelova SK, Kuerten S, Sinis N, Dunlop SA, Angelov DN. 2008. Manually-stimulated recovery of motor

function after facial nerve injury requires intact sensory input. Exp Neurol 211:292–300.

Prescott TJ, Diamond ME, Wing AM. 2011. Active touch sensing. Phil Trans R Soc B 366:2989–2995.

Rinker GC. 1954. The comparative myology of the mammalian genera Sigmodon, Oryzomys, Neotoma, and Peromyscus (Cricetinae), with remarks on their intergeneric relationships. Misc Publ Mus Zool Univ Mich 83:1–125.

Ryan JM. 1989. Comparative myology and polygenetic systematics of the Heteromyidae (Mammalia, Rodentia). Misc Publ Mus Zool Univ Mich 176:1–103.

Sachdev RNS, Sato T, Ebner FF. 2002. Divergent movement of adjacent whiskers. J Neurophysiol 87:1440–1448.

Sherman D, Oram T, Deutsch D, Gordon G, Ahissar E, Harel D. 2013. Tactile modulation of whisking via the brainstem loop: statechart modeling and experimental validation. PLoS ONE 8: e79831.

Silverman RT, Munger BL, Halata Z. 1986. The sensory innervation of the rat rhinarium. Anat Rec 214:210–225.

Sinis N, Horn F, Genchev B, Skouras E, Merkel D, Angelova SK, Kaidoglou K, Michael J, Pavlov S, Igelmund P, Schaller HE, Irintchev A, Dunlop SA, Angelov DN. 2009. Electrical stimulation of paralyzed vibrissal muscles reduces endplate reinnervation and does not promote motor recovery after facial nerve repair in rats. Ann Anat 191:356–370.

Stamper SA, Roth E, Cowan NJ, Fortune ES. 2012. Active sensing *via* movement shapes spatiotemporal patterns of sensory feedback. J Exp Biol 215:1567–1574.

Venkatraman S, Carmena JM. 2011. Active sensing of target location encoded by cortical microstimulation. IEEE Trans Neural Syst Rehabil Eng 19:317–324.

Wachowiak M. 2011. All in a sniff: olfaction as a model for active sensing. Neuron 71:962–973.

Welker WI. 1964. Analysis of sniffing of the albino rat. Behavior 22: 223–244.

Wineski LE. 1985. Facial morphology and vibrissal movement in the golden hamster. J Morphol 183:199–217.

Wong-Riley M. 1979. Changes in the visual system of monocularly sutured or enucleated cats demonstrable with cytochrome oxidase histochemistry. Brain Res 171:11–28.